Nucleic Acids Research, 2003, Vol. 31, No. 20 **6035–6042**
DOI: 10.1093/nar/gkg779

Solvation change and ion release during aminoacylation by aminoacyl-tRNA synthetases

Rajat Banerjee, Amit Kumar Mandal, Rajesh Saha, Soumi Guha, Soma Samaddar, Anusree Bhattacharyya and Siddhartha Roy*

Department of Biophysics, Bose Institute, P-1/12, C.I.T. Scheme VII M, Calcutta 700 054, India

Received May 20, 2003; Revised August 6, 2003; Accepted August 19, 2003

ABSTRACT

Discrimination between cognate and non-cognate tRNAs by aminoacyl-tRNA synthetases occurs at several steps of the aminoacylation pathway. We have measured changes of solvation and counter-ion distribution at various steps of the aminoacylation pathway of glutamyl- and glutaminyl-tRNA synthetases. The decrease in the association constant with increasing KCl concentration is relatively small for cognate tRNA binding when compared to known DNA–protein interactions. The electro-neutral nature of the tRNA binding domain may be largely responsible for this low ion release stoichiometry, suggesting that a relatively large electrostatic component of the DNA–protein interaction free energy may have evolved for other purposes, such as, target search. Little change in solvation upon tRNA binding is seen. Non-cognate tRNA binding actually increases with increasing KCl concentration indicating that charge repulsion may be a significant component of binding free energy. Thus, electrostatic interactions may have been used to discriminate between cognate and non-cognate tRNAs in the binding step. The catalytic constant of glutaminyl-tRNA synthetase increases with increasing osmotic pressure indicating a water release of 8.4 ± 1.4 mol/mol in the transition state, whereas little change is seen in the case of glutamyl-tRNA synthetase. We propose that the significant amount of water release in the transition state, in the case of glutaminyl-tRNA synthetase, is due to additional contact of the protein with the tRNA in the transition state.

INTRODUCTION

Correct aminoacylation of cognate tRNAs by aminoacyl-tRNA synthetases (aaRSs) is perhaps the most important step in translation of mRNA code to the linear sequence of amino acids with high fidelity. *In vivo*, the aaRSs have to achieve a high degree of specificity in aminoacylation in the presence of many non-cognate tRNAs presenting similar conformational features (1). This high degree of specificity is a result of direct interactions and indirect conformational preferences of different nucleo-bases present in different tRNAs. It is likely that all the bases do not play an important role in imparting an 'identity' on a tRNA. Those bases which are important in determining the identity of a tRNA in terms of correct aminoacylation have been termed 'identity elements' and have been mapped for several tRNAs (2).

Mechanistically, how these identity elements increase aminoacylation rate, is not completely understood. Their influence may occur at several stages: (i) at the initial binding level, (ii) at the catalysis level or (iii) at the post catalysis step, i.e. editing (3). Although editing is probably an important feature of some aaRSs, it is unlikely to be of general importance. The binding and catalysis steps can be separated in a formal sense and the importance of each step can be elucidated in the process. The nature of the ground states and the transition states along the aminoacylation pathway has to be elucidated for a proper understanding of the structural basis of discrimination between cognate and non-cognate tRNAs.

One of the ways to investigate the nature of the transition states and ground states is to study the effect of ionic strength and solvation on different steps of aminoacylation. A number of workers have investigated ion and water release that occurs upon protein–DNA interaction (4,5). In the case of regulatory proteins, ion and water release upon binding of a protein to specific DNA sequence constitutes a major driving force. On the other hand, very little water release occurs upon binding of these proteins to non-specific DNA sequences, which is driven primarily by ion release (6). It has been suggested that the water release in the specific complexes may occur because of direct, specific hydrogen bonding of protein side-chains with the polar atoms in the major and minor grooves of DNA, which does not occur in the non-specific complexes. In addition, catalytic steps of restriction endonucleases have been probed for water release using neutral osmolytes. Sligar and co-workers have looked at the dependence of the catalytic constant (k_{cat}) upon osmotic pressure to infer solvation changes in the transition state (7,8).

Clearly, use of such techniques to study ion and water release in the ground and transition states of aminoacylation would yield important information about how the specificity of aminoacylation is achieved. The initial binding step of tRNA and aaRS interaction has been studied for several cognate tRNAs and their mutants, primarily by derivation of

*To whom correspondence should be addressed. Tel: +91 33 2355 0254; Fax: +91 33 2334 3886; Email: sidroy@vsnl.com

K_M through steady-state kinetics (9,10). A study of direct equilibrium binding of tRNAs with aaRSs as a function of salt or osmolyte concentration can provide a wealth of information about ion distribution and solvation change. This in turn can provide information on the nature of the forces involved in tRNA–aaRS complexes. More importantly, knowledge about the transition state can be derived by studying the effect of salt and osmolytes on k_{cat}. Due to its transient nature, these types of indirect techniques are the only ones available for elucidation of the nature of the transition state.

In this work, we have studied ion and water release that occurs upon binding of $tRNA^{gln}$ and $tRNA^{glu}$ to their cognate aaRSs, glutaminyl and glutamyl-tRNA synthetase from *Escherichia coli,* which are closely related. We have also studied the solvation changes in the transition state of the rate-determining step of the aminoacylation reaction.

MATERIALS AND METHODS

Materials

$tRNA^{glu}$, ATP, L-glutamic acid and Sephadex G-25 were purchased from Sigma Chemical Co. (St Louis, MO, USA). The measured specific activity of $tRNA^{glu}$ was ~1.5 nmol/A_{260} and was used without further purification. All other chemicals were of analytical grade.

Methods

Glutamyl-tRNA synthetase (GluRS) purification. Purification of GluRS was carried out according to Brisson *et al.* (11). The specific activities were comparable to those reported in 11.

Glutaminyl-tRNA synthetase (GlnRS) purification. GlnRS was purified according to Hoben *et al.* (12) with some minor modifications as described by Bhattacharyya *et al.* (13). Enzyme assays are also described in the same article. The protein preparation showed a single band on SDS polyacrylamide gel and had specific activities comparable to those reported in 13.

$tRNA^{Gln}$ purification. Cells harboring pRS3 were grown according to the method described by Perona *et al.* (14) and $tRNA^{gln}$ was purified from harvested cells using the methodology described in Bhattacharyya *et al.* (13). Specific activities of ~2 nmol/A_{260} units were obtained.

$tRNA^{Glu}$ purification. Escherichia coli (DH5α) containing pKR15 plasmid (15) was grown overnight in Luria–Bertani broth medium supplemented with 100 µg/ml ampicillin at 37°C. Cells were pelleted down at 5000 r.p.m. for 15 min. Cells (12 g) were resuspended in 20 ml buffer E (10 mM magnesium acetate, 10 mM Tris–HCl, pH 7.2). To 20 ml cell suspension, an equal volume of phenol (saturated with 10 mM Tris–HCl, 1 mM EDTA, pH 7) was added and shaken for 30 min in a dark environment. The phenol layer was extracted thrice. The aqueous layers were pooled and 2.5 vol ice-cold isopropanol was added and kept at –20°C overnight. The precipitate was pelleted down at 4°C for 25 min at 14 000 r.p.m. The pellet was then resuspended in another buffer (0.2 M Tris–HCl, pH 9) at room temperature under sterile conditions. The solution was again centrifuged at 4°C for 10 min at 14 000 r.p.m. and the supernatant was removed.

The supernatant was then loaded onto a 20 ml DE-52 column, which was already equilibrated with buffer F (0.02 M Tris–HCl, pH 7.5 containing 0.2 M NaCl, 0.001 M EDTA, 0.01 M magnesium chloride and 0.002 M sodium thiosulphate). After loading, the column was washed with the same buffer and then eluted with a linear gradient from 0.2 to 0.9 M NaCl in the same buffer at a flow rate of 1 ml/min. The $tRNA^{Glu}$ activity was eluted near 0.4 M NaCl. The specific activity of pure fractions was above 1.5 nmol/A_{260} unit.

Surface area calculation. Surface area calculation was done using appropriate PDB coordinates with the GETAREA program from the University of Texas (http://www.scsb.utmb.edu/getarea/area_man.html#references).

NMR methods. All NMR spectra were obtained in a Bruker DRX-500 spectrometer using the WATERGATE water suppression method. All NMR experiments were conducted in 10 mM potassium phosphate buffer, pH 7.5 containing 10 mM $MgCl_2$ and 1 mM EDTA at 27°C.

Fluorescence methods. Steady-state fluorescence was measured in a Hitachi F3010 spectrofluorometer. The temperature was controlled by circulating water at appropriate temperatures through the chamber and the cuvette holder. The excitation and emission band passes were 5 nm, unless stated otherwise. Spectra of appropriate buffers were always subtracted from the fluorescence spectra.

Binding of tRNA to aaRSs by tryptophan fluorescence quenching was carried out at 25°C. For GlnRS, the buffer was 10 mM Tris, pH 7.5 containing different concentrations of KCl, with or without 5 mM $MgCl_2$. In the case of solvation change measurements with triethylene glycol (TEG), the buffer was 100 mM Tris–HCl buffer, pH 7.5 containing 2.5 mM ATP and 15 mM $MgCl_2$ or without ATP and $MgCl_2$. The bandpasses were 3 and 5 nm for excitation and emission, respectively. For GluRS titrations, the buffer was 10 mM HEPES pH 7.2, containing 5 mM $MgCl_2$. The excitation was at 295 nm and the emission wavelength was 340 nm. Fluorescence at each point was measured separately. The fluorescence of the protein at a concentration of 0.2 µM was determined first. A pre-determined concentration of tRNA was added to that and after ~1 min, the fluorescence was determined again. The inner filter effect was corrected using the following formula:

$$F_{corr} = F_{obs} \text{ antilog } [(A_{ex} + A_{em})/2]$$

The ratio of the corrected fluorescence intensities was used as a measure of quenching. The data were fitted to a single site binding equation, using Kyplot (Koichi Yoshioka, 1997–1999, version 2.0 beta 4). At least four experiments were done under all conditions and average values and standard deviations were used to construct the plots. In order to calculate cation release stoichiometry, GlnRS/$tRNA^{Gln}$ binding parameters in the presence of KCl were fitted to the above equation. Water release stoichiometry was calculated from the slope of $\log_{10} K_{obs}$ versus [TEG] plot, as developed by Garner and Rau (4).

$$\frac{d\log_{10}(K_{obs})}{d[\text{Triethylene glycol}]} = -\frac{2.303\,\Delta n_w}{55.5}$$

where Δn_W is the change in the number of solute-excluding water molecules coupled to GlnRS/tRNA^{Gln} binding.

k_{cat} calculation and $\Delta v^{\neq}$ determination

Enzyme assays were performed as described previously (13), except that substrates were kept at saturating concentrations, at different ethylene glycol concentrations from 0 to 3 M to achieve the desired osmolalities. Osmotic pressures (π) were calculated, according to equation $\pi = RT[O_s]$, where $[O_s]$ includes the concentration of all ionic and neutral osmolytes present. k_{cat}, the catalytic constant, was calculated from the slope of the product formed versus time plot. The substrates were kept at saturation levels to avoid any K_M effect.

Activation volume, $\Delta v^{\neq}$, was calculated using the slope of plot $\ln(k_{cat}[\pi]/k_{cat}[0])$ versus osmotic pressure, π, by applying the relation

$$\frac{\delta \ln k_{Cat}}{\delta \pi} = \frac{\Delta v^{\neq}}{RT}$$

where R is the gas constant, and T is temperature. Solvation change was calculated according to Lynch and Sligar (7).

RESULTS

Ion release resulting from protein–DNA interaction has been studied from the dependence of binding equilibrium on ionic strength. A similar technique is used here for tRNA–aaRS interaction. Figure 1 shows a log–log plot of association constants versus KCl concentrations for GlnRS/tRNA^{Gln} interaction in the absence of $MgCl_2$. The plot shows a monotonic decrease in affinity with increasing KCl concentration. The slope of the line corresponds to a cation release stoichiometry of 1.3 ± 0.3. Since *in vivo*, magnesium is always present, we have determined the cation release stoichiometry in the presence of magnesium (inset). A value of 1.31 ± 0.12 was obtained in the presence of 5 mM $MgCl_2$. These values for tRNA–aaRS interaction are much smaller than reported for several protein–DNA interactions. This low cation release stoichiometry was also qualitatively verified by fluorescent 5-({[(2-iodoacetyl)amino]ethyl}amino) naphthalene-1-sulfonic acid (IAEDANS) modified tRNA^{Gln}. The cation release stoichiometry was found to be 0.93 ± 0.3 even for a modified tRNA, suggesting qualitative agreement (data not shown). We have explored the generality of the previous results by studying another tRNA–aaRS interaction. GluRS is the most closely related aaRS to GlnRS. Figure 1 also shows the log K_a versus log [MX] plot for GluRS/tRNA^{Glu} system from *E.coli* in buffers containing 5 mM $MgCl_2$. 5 mM $MgCl_2$ was included in all tRNA^{Glu} experiments as it is well known that the tRNA is non-functional without relatively high Mg^{2+} concentrations (16). The slope of the plot is similar to the GlnRS/tRNA^{gln} plot with an ion release value of 1.7 ± 0.22. In lac repressor, Record and co-workers have estimated a cation release stoichiometry of ~8 upon lac repressor dimer binding to operator (17) indicating that the role of electrostatics in tRNA–aaRS interaction is qualitatively different from that in the DNA–protein interactions.

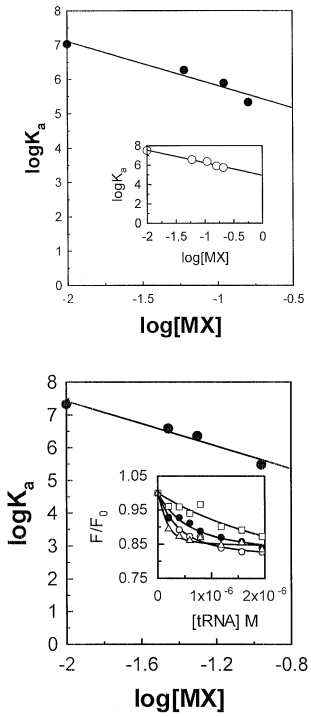

Figure 1. Ionic strength dependence of aaRS–tRNA interaction. Upper panel, log–log plot of association constant versus monovalent ion concentration of GlnRS/tRNA^{Gln} interaction. The experiments were conducted in 10 mM Tris–HCl buffer, pH 7.5 at 25°C. Inset shows the same plot in the presence of 5 mM $MgCl_2$. Lower panel, plot of log association constant versus log monovalent ion concentration of GluRS/tRNA^{Glu} interaction. The experiments were conducted in 10 mM HEPES buffer, pH 7.2 containing 5 mM $MgCl_2$ at 25°C. The inset shows the actual quenching curves at 0 (open triangles), 25 (open circles), 50 (filled circles) and 100 mM KCl (open squares). Association constants were determined by quenching of tryptophan fluorescence as described in Methods. The excitation wavelength was 295 nm and emission wavelength was 340 nm. The protein concentration was 0.2 μM. Each point is an average of four independent titrations. The average standard error for each point is ~1%. The error bars are not shown as they lead to crowding.

Neutral osmolytes have been widely used to estimate solvation changes that occur during protein–DNA complex formation. Figure 2 shows a plot of log association constant as a function of a neutral osmolyte, TEG. The inset shows the fluorescence quenching at two different TEG concentrations. The association constant increases modestly as the concentration of TEG is increased up to 1.5 M, indicating a modest amount of water release upon complex formation. The slope of the line indicates 0–4 mol/mol of water is released when the tRNA–aaRS complex is formed. Since Mg^{2+} is known to bind to tRNA with high affinity at some pockets, we have also investigated whether the presence of Mg^{2+} in any way reduces the water release stoichiometry. The water release is significantly higher in the absence of Mg^{2+} (~10–15 water molecules). However, even this increased number is much smaller than the water release that occurs upon specific protein–DNA complex formation. We have also examined the solvation change that occurs upon interaction of tRNA^{Glu} with GluRS. Figure 2 also shows the plot of [TEG] versus

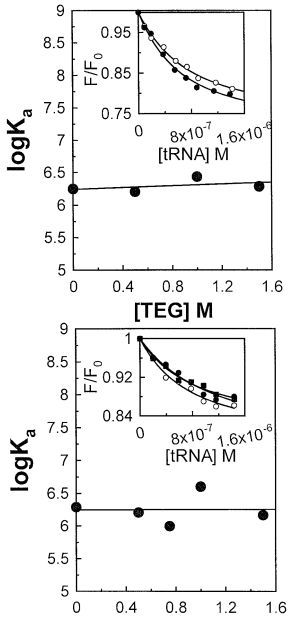

Figure 2. TEG concentration dependence of tRNA–aaRS interaction. Upper panel, plot of log association constant versus [TEG] of GlnRS/tRNA^{Gln} interaction. The experiments were conducted in 100 mM Tris–HCl buffer, pH 7.5 containing 2.5 mM ATP and 15 mM $MgCl_2$ at 25°C. The inset shows the actual quenching curves at 0.5 M (open circles) and 1.5 M TEG (filled circles). Lower panel, plot of log association constant versus [TEG] of GluRS/tRNA^{Glu} interaction. The experiments were conducted in 10 mM HEPES buffer, pH 7.2 containing 5 mM $MgCl_2$ at 25°C. The inset shows the actual quenching curves at 0.5 M (open circles), 0.75 M (filled circles) and 1.5 M TEG (filled squares). Association constants were determined by quenching of tryptophan fluorescence as described in Methods. The excitation wavelength was 295 nm and emission wavelength was 340 nm. The protein concentration was 0.2 µM. Each point is an average of four independent titrations. For error analysis, see the legend of Figure 1.

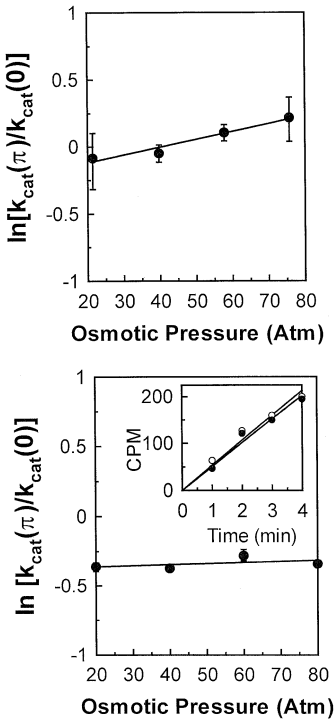

Figure 3. Upper panel, osmotic pressure dependence of k_{cat} for aminoacylation of tRNA^{Gln} by GlnRS. The assays were conducted in 50 mM potassium phosphate buffer, pH 7.0 containing 5 µM tRNA^{Gln}, 500 µM L-glutamine, 2.5 mM ATP and 12.5 mM $MgCl_2$ at 37°C. Lower panel, osmotic pressure dependence of k_{cat} for aminoacylation of tRNA^{Glu} by GluRS. The assays were conducted in 50 mM HEPES buffer, pH 7.2 containing 0.8 mM 2-mercaptoethanol, 5 µM tRNA^{Glu}, 500 µM L-glutamate, 2 mM ATP and 16 mM $MgCl_2$ at 37°C. The inset shows the linearity of the assays at two different atmospheric pressures. Five sets of assays were performed in the presence of different concentrations of ethylene glycol. Each point is the average of four independent measurements.

association constant for GluRS/tRNA^{Glu} system in the presence of magnesium. Again, like the GlnRS/tRNA^{Gln} system, the water release is between 0 and 4 mol/mol upon complex formation.

The rate-determining step in the aminoacylation pathway appears to be the transfer of activated amino acid to the 3′ hydroxyl group of the terminal A76 (18,19). We have investigated solvation changes in the transition state by studying the dependence of k_{cat} on osmotic pressure. Figure 3 shows the plot of $\ln[k_{cat}/k°_{cat}]$ versus osmotic pressure for the GlnRS/tRNA^{Gln} system. The plot shows reasonable linearity and the slope translates to a water release stoichiometry of 8.4 ± 1.4 mol/mol. This indicates that additional surface area becomes buried in the transition state, the measure of which is probably dependent upon the degree of solvation in the previous ground state. Although this burial of surface area can occur within the protein or the tRNA, a distinct possibility is that this occurs because of additional contact between the tRNA and the protein. This transient contact during the transition state will lead to stabilization of the transition state and rate enhancement of aminoacylation. It has been shown that mutations in some identity elements lead to significant lowering of k_{cat} (increase in activation energy). The identity elements may thus act by lower the activation energy at the rate-determining step (20). It is likely that this lowering of activation energy occurs because of transient contact of these bases with protein atoms during the transition state. To test another tRNA–aaRS pair, we have investigated solvation changes in the transition state by studying the dependence of k_{cat} of aminoacylation of tRNA^{Glu} by GluRS, on osmotic pressure. Figure 3 also shows the plot of $\ln[k_{cat}(\pi)/k_{cat}(0)]$ versus osmotic pressure for the tRNA^{Glu}–GluRS pair. The plot shows reasonable linearity and the slope translates to a water release stoichiometry of ~1 mol/mol. This would indicate very little burial of additional surface area from the solvent in the transition state. Although this small solvation change can be interpreted as no additional contact in the transition state, it cannot completely rule out the possibility of additional contact, since burial of surface areas may not always lead to significant solvation change.

In the cellular milieu, an aaRS has to reject many non-cognate tRNAs with a high degree of accuracy. It appears that in at least one case, the K_M difference is fairly large between a non-cognate and cognate tRNA (21). Since very little structural information on the non-cognate complex is available, we have used the techniques described above to investigate ion release and solvation changes that occur upon non-cognate complex formation. Figure 4 shows the ionic strength dependence of log K_a of tRNA^{Gln}/GluRS

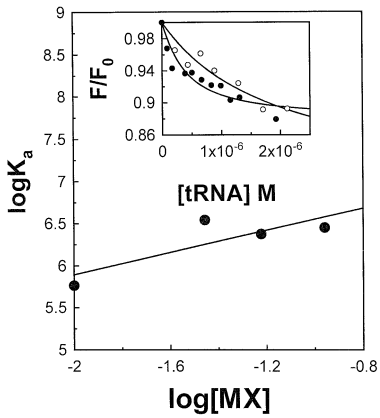

Figure 4. Ionic strength dependence of non-cognate GluRS/tRNA^{Gln} interaction. Log–log plot of association constant versus monovalent ion concentration of GluRS/tRNA^{Gln} interaction. The experiments were conducted in 10 mM HEPES buffer, pH 7.2 containing 5 mM $MgCl_2$ at 25°C. Association constants were determined by quenching of tryptophan fluorescence as described in Methods. The excitation wavelength was 295 nm and emission wavelength was 340 nm. The protein concentration was 0.2 μM. Each point is the average of four independent titrations. The inset shows the actual quenching curves at 0 M (open circles) and 25 mM KCl (filled circles).

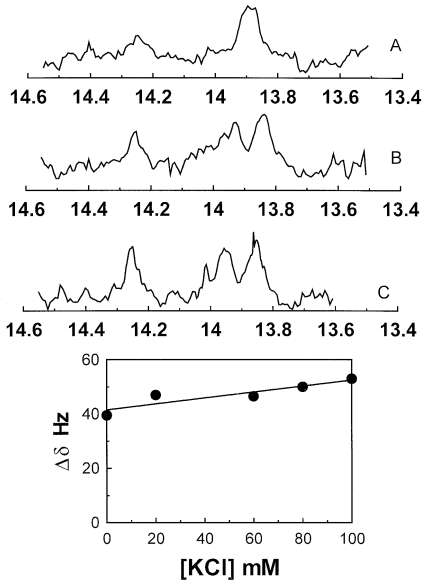

Figure 5. NMR spectra of (**A**) 148 μM tRNA^{Gln}, (**B**) 148 μM tRNA^{Gln} and 148 μM GluRS and (**C**) the same as (B) except the buffer contained 100 mM KCl at 27°C. The lower panel shows the plot of difference of chemical shift of the two shifting peaks (at around 13.8 p.p.m.) versus KCl concentration. 5000–8000 scans were signal averaged in 8 mm sample tubes to enhance the signal-to-noise ratio. The solution conditions were 10 mM potassium phosphate, pH 7.5 containing 10 mM $MgCl_2$ and 1 mM EDTA.

interaction. In contrast to the cognate pair, affinity increases with increasing ionic strength.

We have attempted to verify this trend qualitatively by another technique. Figure 5 shows a region of the imino proton spectrum of tRNA^{Gln} in the presence and absence of a stoichiometric amount of GluRS. One of the resonances in the free tRNA^{Gln} (actually composed of two resonances) splits upon non-cognate complex formation. These resonances are likely to be AU base pairs because of their chemical shift (22). When tRNA^{Gln} was gradually titrated with GluRS up to 1:1 stoichiometry, the chemical shift difference gradually increased (data not shown). Addition of 100 mM KCl to the complex does not cause any decrease in the chemical shift difference (Fig. 5, bottom). Under a similar situation, the dissociation constant of non-specific protein–DNA interaction is increased by several orders of magnitude. Although the GluRS and tRNA^{Gln} concentrations are approximately two orders of magnitude higher than the dissociation constant of the complex, an increase in dissociation constant of similar magnitude as above would lead to dissociation of the complex and consequently the disappearance of the splitting. Even the dissociation constant of cognate GluRS/tRNA^{Glu} changes by approximately two orders of magnitude under similar conditions. A similar behavior in the non-cognate case would have lead to significant convergence of the two resonances. Thus it is likely that the salt sensitivity of the GluRS/non-cognate tRNA interaction is even less than the GluRS/cognate interaction. This is consistent with the results stated before. Figure 6 shows the plot of log K_a versus TEG concentration. The plot, like that of the cognate case, is essentially flat, indicating little solvation changes.

All ion and water release stoichiometries are summarized in Table 1.

DISCUSSION

Results obtained in this study suggest little solvation change and low ion release stoichiometry upon tRNA–aaRS complex formation, which in turn suggests that unlike the DNA–protein counterpart, ion and water release only weakly contribute to

Table 1. Ion and water release stoichiometry for different tRNA–aaRS pairs

tRNA/synthetase pair	Conditions	Ion stoichiometry	Water stoichiometry
tRNA/GlnRS	No Mg	1.3 ± 0.3	
	5 mM Mg	1.31 ± 0.12	
	No Mg or ATP		11–15
	15 mM Mg and ATP		0–4
tRNA^{Glu}/GluRS	5 mM Mg	1.7 ± 0.22	
	5 mM Mg		0–4
tRNA^{Gln}/GluRS	5 mM Mg	<0	
	5 mM Mg		~0
tRNA^{Gln}/GlnRS (transition state)			8.4 ± 1.4
tRNA^{Glu}/GluRS (transition state)			~0

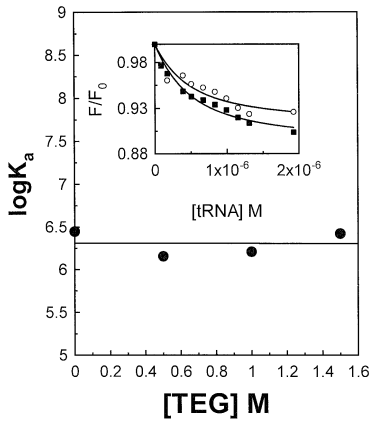

Figure 6. TEG concentration dependence of non-cognate GluRS/tRNA^{Gln} interaction. Plot of log association constant versus [TEG] of GluRS/tRNA^{Gln} interaction. The experiments were conducted in 10 mM HEPES buffer, pH 7.2 containing 5 mM $MgCl_2$ at 25°C. Association constants were determined by quenching of tryptophan fluorescence as described in Methods. The excitation wavelength was 295 nm and emission wavelength was 340 nm. The protein concentration was 0.2 µM. Each point is the average of four independent titrations. The inset shows the actual quenching curves at 0 M (open circles) and 1.5 M TEG (filled squares).

the free energy of interaction in the tRNA–aaRS system. One major concern about interpreting these results in terms of nature of the interaction is the question of folding–unfolding transitions coupled to binding. In the cases of both GlnRS and GluRS (*Thermus thermophilus*, a homologue of the *E.coli* enzyme), both free and tRNA bound structures are now known and seem to rule out any major folding/unfolding event in the protein upon tRNA binding (23–25). Conformational change in tRNA due to aaRS binding is less well documented since the structure of the free tRNA^{Gln} is not known. If the free conformation of tRNA^{Gln} is assumed to be like that of the yeast tRNA^{Phe}, then significant change occurs at the CCA end and the anticodon loop upon binding to the aaRS. The exposed surface area of yeast tRNA^{Phe} (crystal structure conformation) differs from the bound tRNA^{Gln} conformation by more than 200 Å^2 and most of this change occurs in the regions through which the tRNA interacts with the aaRS. However, due to relatively small changes in the tRNA and aaRS structure upon complex formation (compared to the surface area buried upon complex formation), it is unlikely that a coupled folding event could entirely account for the low stoichiometry of ion and water release.

The magnitude of the ionic strength effects is highly dependent on the electrostatic interactions between negatively charged phosphates and the charged groups of the protein. The best characterized protein–nucleic acid interaction with respect to ion and water release is perhaps the lac repressor/operator complex. Dependence of binding constant as a function of monovalent salt and osmolyte is relatively large and can be interpreted as equivalent to release of eight cations and 200 water molecules upon lac repressor dimer binding to lac operator. In the process, ~3600 Å^2 surface area becomes buried. Figure 7A shows the crystal structure of the lac repressor–operator complex in which only protein heavy-atoms within 4.5 Å of the phosphorus atoms are shown; 4.5 Å was chosen as a cut-off as any group which hydrogen bonds with the DNA phosphates will be within that distance from the phosphorus atoms. As can be seen from the figure, groups from the lac repressor protein closely approach approximately eight phosphates. This is close to the number of cations released obtained from the ionic strength dependence of the association constant. Figure 7B shows the picture of tRNA^{Gln} as approached by atoms of GlnRS using the same cut-off as above. Eight phosphates are closely approached by atoms from GlnRS. Six of these groups are positively charged lysine and arginine. This number is expected to contribute significantly to the ionic strength dependence of the association constant. The crystal structure of the tRNA^{Glu}/GluRS (*T.thermophilus*) complex suggests that about seven phosphates are closely approached by protein heavy atoms (data not shown). Thus one may expect relatively high salt dependence of interaction energy in the tRNA–aaRS systems studied here (24,25).

However, the dependence of the tRNA–aaRS interaction in the GlnRS and GluRS system upon addition of monovalent salt is very low. A significant part of the explanation for lower salt dependence of the binding free energy lies in the overall charge distribution of the interacting surfaces of the proteins. In the lac repressor, there are overall 14 positively charged groups and three negatively charged groups within 10 Å of the phosphate, giving the DNA binding domain a highly positively charged character (Fig. 7C). All 14 positively charged groups are within 8 Å of the phosphates, whereas the three negatively charged groups are within 8–10 Å of the phosphates. In contrast, in the GlnRS/tRNA^{Gln} complex, 21 positively charged groups and 17 negatively charged groups are within 10 Å of the phosphates (Fig. 7D) and 17 positively charged and 14 negatively charged groups are within 8 Å of the phosphates. This gives the tRNA binding interface a much more electroneutral character and probably much lower salt dependence of the binding free energy. Recently, Norberg (26) has calculated the salt-dependent part of the free energy for several protein–DNA complexes. In most cases, the protein has an overall positive charge except for BamHI and MetJ repressor. The salt-dependent part of the free energy is generally high for most of the complexes except for MetJ and BamHI. The salt dependence of the calculated free energy is also low for the latter two complexes compared to others, thus supporting our conclusions.

Does the low electrostatic contribution to the overall free energy of RNA–protein interaction occur in other RNA–protein systems? To our knowledge, there are three other studies of salt effect on protein–RNA interactions. Florentz *et al.* (27), have also reported enhanced binding of tRNA^{Val} to ValRS at relatively high concentrations of another cosmotropic salt, ammonium sulfate—which they suggested to be due to the hydrophobic component of the interaction. Very weak salt dependence was observed by Altman and coworkers for RNA–protein interaction in Ribonuclease P (28). Weak salt dependence of Chandipura virus leader RNA binding to P-protein was also observed (S.Basak, D.J.Chattopadhyay and S.Roy, unpublished observation). Unlike DNA–protein interactions, weak salt dependence and consequent low salt-dependent free energy may be a characteristic of many RNA–protein interactions. The relatively large contribution of electrostatic free energy in DNA–protein

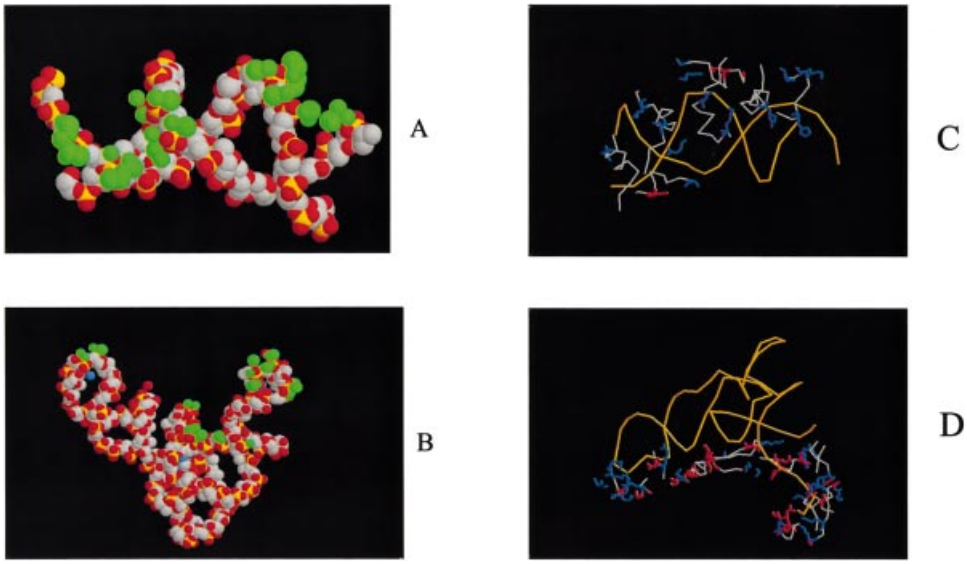

Figure 7. Protein heavy-atoms (in green) within 4.4 Å of phosphorus atoms of (**A**) lac operator and (**B**) $tRNA^{Gln}$ in a GlnRS/$tRNA^{Gln}$/ATP complex. Cationic (blue) and anionic (red) residues within 10 Å of the (**C**) DNA phosphates in a lac operator/repressor complex and (**D**) tRNA phosphates in a GlnRS/$tRNA^{Gln}$ complex. The pictures were generated in RASMOL using crystallographic coordinates obtained from RCSB (1EFA for lac repressor/operator and 1qtq for GlnRS/$tRNA^{Gln}$).

interaction may have evolved for other processes, such as, target search.

Electrostatic forces probably play a very important role in non-cognate tRNA discrimination as well. Discrimination of non-cognate tRNA probably occurs at several steps and a significant component may be present at the initial binding step. Lack of requirement of a large electrostatic component of free energy in RNA–protein interaction may allow electrostatic interactions to be used in tRNA–aaRS interaction differently, e.g. in discrimination of non-cognate tRNAs. It has been demonstrated that Glu152 in TyrRS and Asp449 and Asp456 in MetRS disproportionately decrease binding of non-cognate tRNAs by charge repulsion (29,30). Enhanced binding of non-cognate tRNA at higher salt concentrations reported here may suggest a similar mechanism is used by the GlnRS. Thus electrostatic repulsion of non-cognate tRNAs may be a general mechanism of discrimination.

The origin of the low water release stoichiometry upon complex formation is not clearly understood. The effect of osmolyte, TEG, on protein structure is ruled out as TEG has little effect on CD, fluorescence and equilibrium denaturation of GlnRS (31). Another osmolyte, L-glutamate, also showed very low ion and water release, suggesting the general nature of the results (data not shown). For comparison with the lac repressor system, if one calculates the surface area that is buried upon complex formation (excluding any conformational change), it translates to 3600 $Å^2$ in the case of the lac repressor/operator interaction and 5200 $Å^2$ for the GlnRS/$tRNA^{Gln}$ interaction (23). It would be anticipated that water release should be in the order of 200 or more for the GlnRS/$tRNA^{Gln}$ interaction if the same type of solvation is assumed in both cases. We have also calculated the surface area change upon binding of $tRNA^{Glu}$ to GluRS (*T.thermophilus*). The calculated surface area change is like that of the GlnRS system (4300 Å2). Although little is known about the structural detail of the hydration layer of proteins, it is possible that the nature of the surface buried may be related to water release. Another possible explanation of much reduced water release may lie in the coupled conformational change in the tRNA molecule. If the free $tRNA^{Gln}$ molecule is similar in structure to that of the yeast $tRNA^{Phe}$ in crystal, then the main interacting regions, CCA end and the anti-codon bases are all stacked in the free state. Thus, the bases are likely to be desolvated significantly in the free state and hence binding to a protein pocket may not lead to significant release of water molecules. Similarly, hydrophobic pockets into which these bases bind may not be solvated significantly. The water release is so high in lac repressor/operator interaction probably because the interaction occurs primarily through a major groove of the DNA, which may be fairly polar and highly hydrated.

One of the ways one can obtain information about the difference between the transition state and the preceding ground state is by measuring solvation differences. Higher water release in the transition state of GlnRS strongly argues for more burial of the surface area. How much of the surface area is buried, probably depends on the region and types of interaction that occur. Whether this occurs within protein or between protein and nucleic acid cannot be stated with certainty. Previously a number of workers have postulated base specific contacts in the transition state as a mechanism for enhancement of aminoacylation rate for the cognate tRNA (20,32). All these studies were based on lowering of k_{cat} by mutations in the tRNA, distant from the active site. Given that additional significant solvation change occurs in the transition state, it is likely that this influence is exerted through additional interaction of the identity elements of the tRNA

with the protein. Interestingly, in the case of GluRS, very little water is released, indicating either no additional contact or contacts of qualitatively different nature in the transition state.

CONCLUSION

The contribution of the electrostatic component in tRNA–aaRS interaction is much smaller that its protein–DNA counterpart possibly due to the more electroneutral nature of the protein interaction domains. Amongst other possibilities, the presence of many negative charges in the interacting domain and consequent electroneutrality may have evolved so as to use charge repulsion for non-cognate discrimination at the binding step. Enhanced discrimination between the cognate and the non-cognate tRNA at the catalytic step may involve additional contact with the cognate substrate.

ACKNOWLEDGEMENTS

We thank Professor V. K. Misra for very useful discussion. We also thank CSIR, Government of India for funding this research and providing fellowships for R.S., S.S. and S.G.

REFERENCES

1. Soll,D. (1990) The accuracy of aminoacylation—ensuring the fidelity of the genetic code. *Experientia*, **46**, 1089–1096.
2. Giege.,R., Sissler,M. and Florentz,C. (1998) Universal rules and idiosyncratic features in tRNA identity. *Nucleic Acids Res.*, **26**, 5017–5035.
3. Ibba,M. and Soll,D. (1999) Quality control mechanisms during translation. *Science*, **286**, 1893–1897.
4. Garner,M.M. and Rau,D.C. (1995) Water release associated with specific binding of gal repressor. *EMBO J.*, **14**, 1257–1263.
5. Ha,J.H., Capp,M.W., Hohenwalter,M.D., Baskerville,M. and Record,M.T. (1992) Thermodynamic stoichiometries of participation of water, cations and anions in specific and non-specific binding of lac repressor to DNA. Possible thermodynamic origins of the 'glutamate effect' on protein–DNA interactions. *J. Mol. Biol.*, **228**, 252–264.
6. de Haseth,P.L., Lohman,T.M. and Record,M.T. (1977) Nonspecific interaction of lac repressor with DNA: an association reaction driven by counterion release. *Biochemistry*, **16**, 4783–4790.
7. Lynch,T.W. and Sligar,S.G. (2000) Macromolecular hydration changes associated with BamHI binding and catalysis. *J. Biol. Chem.*, **275**, 30561–30565.
8. Robinson,C.R. and Sligar,S.G. (1998) Changes in solvation during DNA binding and cleavage are critical to altered specificity of the EcoRI endonuclease. *Proc. Natl Acad. Sci. USA*, **95**, 2186–2191.
9. Hayase,Y., Jahn,M., Rogers,M.J., Sylvers,L.A., Koizumi,M., Inoue,H., Ohtsuka,E. and Soll,D. (1992) Recognition of bases in *Escherichia coli* tRNA(Gln) by glutaminyl-tRNA synthetase: a complete identity set. *EMBO J.*, **11**, 4159–4165.
10. Hou,Y.M. and Schimmel,P. (1989) Modeling with *in vitro* kinetic parameters for the elaboration of transfer RNA identity *in vivo*. *Biochemistry*, **28**, 4942–4947.
11. Brisson,A., Brun,Y.V., Bell,A.W., Roy,P.H. and Lapointe,J. (1989) Overproduction and domain structure of the glutamyl-tRNA synthetase of *Escherichia coli*. *Biochem. Cell Biol.*, **67**, 404–410.
12. Hoben,P., Royal,N., Cheung,A., Yamao,F., Biemann,K. and Soll,D. (1982) *Escherichia coli* glutaminyl-tRNA synthetase. II. Characterization of the glnS gene product. *J. Biol. Chem.*, **257**, 11644–11650.
13. Bhattacharyya,T., Bhattacharyya,A. and Roy,S. (1991) A fluorescence spectroscopic study of glutaminyl-tRNA synthetase from *Escherichia coli* and its implications for the enzyme mechanism. *Eur. J. Biochem.*, **200**, 739–745.
14. Perona,J.J., Swanson,R., Steitz,T.A. and Soll,D. (1988) Overproduction and purification of *Escherichia coli* tRNA(2Gln) and its use in crystallization of the glutaminyl-tRNA synthetase-tRNA(Gln) complex. *J. Mol. Biol.*, **202**, 121–126.
15. Sylvers,L.A., Rogers,K.C., Shimizu,M., Ohtsuka,E. and Soll,D. (1993) A 2-thiouridine derivative in tRNAGlu is a positive determinant for aminoacylation by *Escherichia coli* glutamyl-tRNA synthetase. *Biochemistry*, **32**, 3836–3841.
16. Madore,E., Florentz,C., Giege,R. and Lapointe,J. (1999) Magnesium-dependent alternative foldings of active and inactive *Escherichia coli* tRNA(Glu) revealed by chemical probing. *Nucleic Acids Res.*, **27**, 3583–3588.
17. Record,M.T.,Jr, deHaseth,P.L. and Lohman,T.M. (1977) Interpretation of monovalent and divalent cation effects on the lac repressor–operator interaction. *Biochemistry*, **16**, 4791–4796.
18. Kern,D. and Lapointe,J. (1981) The catalytic mechanism of glutamyl-tRNA synthetase of *Escherichia coli*. A steady-state kinetic investigation. *Eur. J. Biochem.*, **115**, 29–38.
19. Lloyd,A.J., Thomann,H.U., Ibba,M. and Soll,D. (1995) A broadly applicable continuous spectrophotometric assay for measuring aminoacyl-tRNA synthetase activity. *Nucleic Acids Res.*, **23**, 2886–2892.
20. Jahn,M., Rogers,M.J. and Soll,D. (1991) Anticodon and acceptor stem nucleotides in tRNA(Gln) are major recognition elements for *E. coli* glutaminyl-tRNA synthetase. *Nature*, **352**, 258–260.
21. Rogers,K.C. and Soll,D. (1993) Discrimination among tRNAs intermediate in glutamate and glutamine acceptor identity. *Biochemistry*, **32**, 14210–14219.
22. Roy,S. and Redfield,A.G. (1983) Assignment of imino proton spectra of yeast phenylalanine transfer ribonucleic acid. *Biochemistry*, **22**, 1386–1390.
23. Sherlin,L.D. and Perona,J.J. (2003) tRNA-dependent active site assembly in a class I aminoacyl-tRNA synthetase. *Structure*, **11**, 591–603.
24. Nureki,O., Vassylyev,D.G., Katayanagi,K., Shimizu,T., Sekine,S., Kigawa,T., Miyazawa,T., Yokoyama,S. and Morikawa,K. (1995) Architectures of class-defining and specific domains of glutamyl-tRNA synthetase. *Science*, **267**, 1958–1965.
25. Sekine,S., Nureki,O., Shimada,A., Vassylyev,D.G. and Yokoyama,S. (2001) Structural basis for anticodon recognition by discriminating glutamyl-tRNA synthetase. *Nature Struct. Biol.*, **8**, 203–206.
26. Norberg,J. (2003) Association of protein–DNA recognition complexes: electrostatic and non-electrostatic effects. *Arch. Biochem. Biophys.*, **410**, 48–68.
27. Florentz,C., Kern,D. and Giege,R. (1990) Stimulatory effect of ammonium sulfate at high concentrations on the aminoacylation of tRNA and tRNA-like molecules. *FEBS Lett.*, **261**, 335–338.
28. Talbot,S.J. and Altman,S. (1994) Kinetic and thermodynamic analysis of RNA–protein interactions in the RNase P holoenzyme from *Escherichia coli*. *Biochemistry*, **33**, 1406–1411.
29. Bedouelle,H. and Nageotte,R. (1995) Macromolecular recognition through electrostatic repulsion. *EMBO J.*, **14**, 2945–2950.
30. Schmitt,E., Meinnel,T., Panvert,M., Mechulam,Y. and Blanquet,S. (1993) Two acidic residues of *Escherichia coli* methionyl-tRNA synthetase act as negative discriminants towards the binding of non-cognate tRNA anticodons. *J. Mol. Biol.*, **233**, 615–628.
31. Mandal,A.K., Samaddar,S., Banerjee,R., Lahiri,S., Bhattacharyya,A. and Roy,S. (2003) Glutamate counteracts the denaturing effect of urea through its effect on the denatured state. *J. Biol. Chem.*, **278**, 36077–36084.
32. Giege,R., Sissler,M. and Florentz,C. (1998) Universal rules and idiosyncratic features in tRNA identity. *Nucleic Acids Res.*, **26**, 5017–5035.